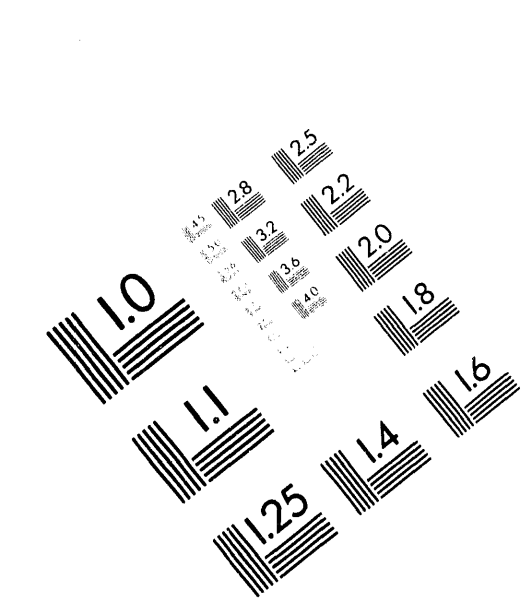

Association for Information and Image Management

1100 Wayne Avenue, Suite 1100
Silver Spring, Maryland 20910

301/587-8202

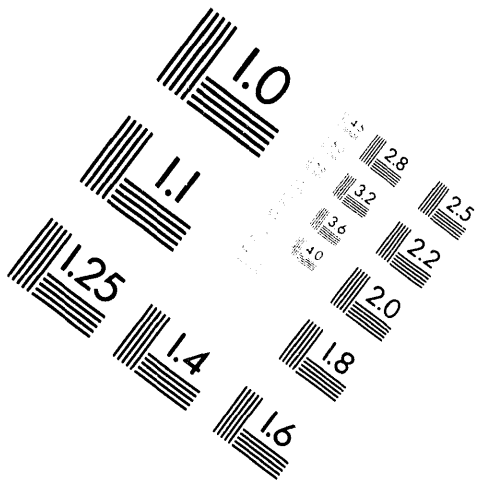

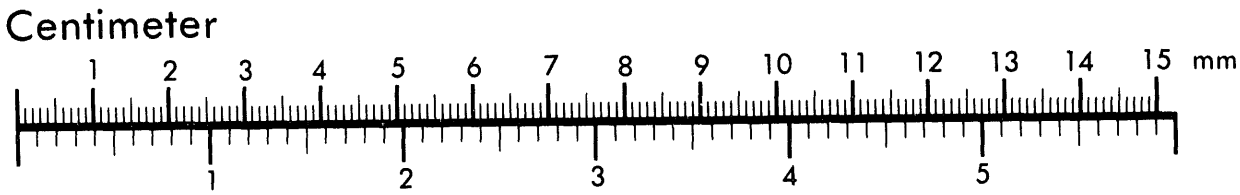

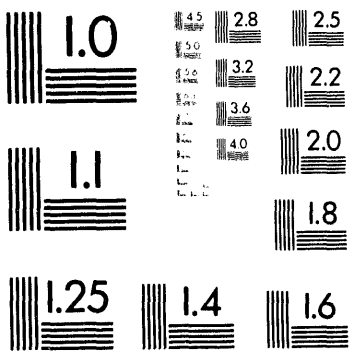

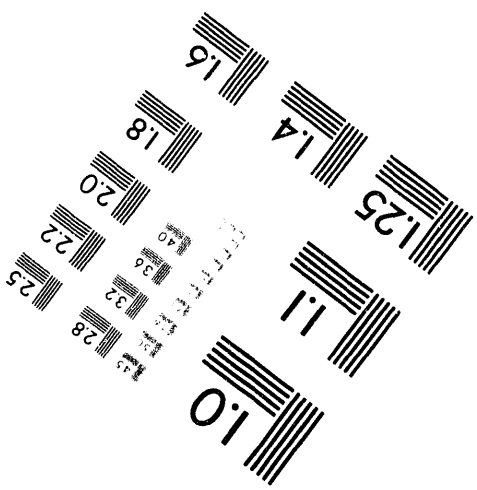

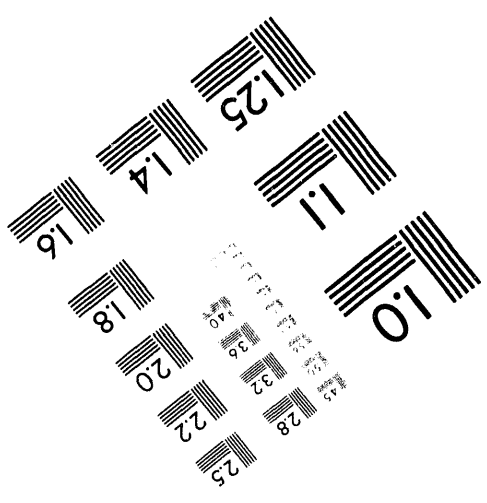

MANUFACTURED TO AIIM STANDARDS
BY APPLIED IMAGE, INC.

1 of 1

ANL/CHM/CP--81410
Conf-940711--16

The Thermal Reactions of CH_3

by

K. P. Lim and J. V. Michael
Chemistry Division, Argonne National Laboratory, Argonne, IL 60439, USA

Corresponding Author: **Dr. J. V. Michael**
D-183, Bldg 200
Argonne National Laboratory
Argonne, IL 60439
Phone: (708) 252-3171, Fax: (708) 252-4470
E-mail: Michael@ANLCHM.BITNET

(25th Symp. (Int'l) on Combust., Submitted Nov., 1993)

Desired Presentation: Oral
Preferred Publication: Proceedings
Code Letter: **E, A** Code Numbers: **1.1, 1.5**

	Text	Reference	Tables	Figures	Total
Count	3545	44 citations	3/4 page	6 pages	
Equiv. Words	3545	783	150	1200	5678

(Not Patentable)

The submitted manuscript has been authored by a contractor of the U. S. Government under contract No. W-31-109-ENG-38. Accordingly, the U. S. Government retains a nonexclusive, royalty-free license to publish or reproduce the published form of this contribution, or allow others to do so, for U. S. Government purposes.

This work was supported by the U. S. Department of Energy, Office of Basic Energy Sciences, Division of Chemical Sciences, under Contract No. W-31-109-Eng-38.

MASTER
DISTRIBUTION OF THIS DOCUMENT IS UNLIMITED
RECEIVED
JUN 10 1994
OSTI

Abstract

The thermal reactions of CH_3-radicals have been investigated in reflected shock waves experiments at temperatures between 1224–2520 K. The fast dissociation of CH_3I served as the source of CH_3. Experiments were performed at three loading pressures with variations in $[CH_3I]_0$. H-atoms formed in the reaction, $2CH_3 \rightarrow C_2H_5 + H$, were measured by the atomic resonance absorption spectrometric (ARAS) technique. The product ethyl radicals subsequently decompose to give a second H-atom and ethylene. A reaction mechanism was used to fit the data, and the resulting value for the rate constant was $5.25 \times 10^{-11} \exp(-7384\ K/T)\ cm^3\ molecule^{-1}\ s^{-1}$. This value is compared to earlier determinations. At higher temperatures, 2150-2520 K, the H-atom formation rate was dominated by CH_3 thermal dissociation. With simulations, the rate constant for $CH_3 + Kr \rightarrow CH_2 + H + Kr$ could be determined. The rate constant for this process is: $k = 4.68 \times 10^{-9} \exp(-42506\ K/T)\ cm^3\ molecule^{-1}\ s^{-1}$. This result is compared to earlier experimental determinations and also to theoretical calculations using the semi-empirical Troe formalism.

INTRODUCTION

The thermal reactions of methyl radicals in the gas phase have been the subject of countless studies during the past forty years. Since the pioneering work of Gomer and Kistiakowsky, [1] there have been over sixty publications on the CH_3 self reactions as noted in the NIST data base. [2] Most of these have been concerned with the low temperature-high pressure measurement of the recombination reaction to form ethane. However, there are several high temperature shock tube studies where the intent has been to measure rate constants for the molecular and atom elimination processes; i. e., $CH_3 + CH_3 \rightarrow C_2H_4 + H_2$ and $CH_3 + CH_3 \rightarrow C_2H_5 + H$, respectively. [3–12]

Warnatz reviewed this earlier work [13] and concluded that the molecular elimination channel had a rate constant of $1.66 \times 10^{-8} \exp(-16117\ K/T)$ cm^3 $molecule^{-1}$ s^{-1} over the temperature range, 1500-2500 K. Following the earlier H-atom atomic resonance absorption spectrometric (ARAS) results of Roth and Just [11] and Roth, [12] Warnatz [13] preferred a value of $1.33 \times 10^{-9} \exp(-13350\ K/T)$ cm^3 $molecule^{-1}$ s^{-1} (1500–3000 K) for the atomic elimination process; however, this has been superseded by a more recent ARAS investigation by Frank and Braun-Unkhoff [14] where a value of $4.6 \times 10^{-11} \exp(-6840\ K/T)$ cm^3 $molecule^{-1}$ s^{-1} between 1320–2300 K was measured. This latter value is more reasonable on theoretical grounds because the A-factor is not inconsistent with that for the back reaction, $H + C_2H_5$, when it is divided by the equilibrium constant. In our own recent work on the thermal decomposition of CH_3Cl, [15] a high value for atomic elimination was obtained for 1550-1900K. The branching ratio between dissociation and elimination continues to be a subject of research. It should be noted that molecular elimination has not been directly observed but only inferred from observations of both precursor (e.g., C_2H_6) and CH_3.

The confusion as to what values to use for the respective processes still persists as seen in recent investigations. Davidson et al. in their C_2H_6 [16] pyrolysis study have

used an earlier value from Just, [17] for molecular elimination. For atomic dissociation, they used the Frank and Braun-Unkhoff [14] value. Kiefer and Kumaran [18] have however used only the Braun-Unkhoff value thereby assuming that molecular elimination was insignificant. Even though $\Delta H^o(0K)$ for molecular elimination is only 30.9 kcal $mole^{-1}$, their assumption may still be sound. If either the 1,2 or 1,1 [19] elimination processes occur through symmetrical transition states then they violate Woodward-Hoffman rules. The transition states would be tight, and either process might then have quite high barrier heights. If these barrier heights are higher than or near to that for atomic dissociation then the molecular process, in an RRK sense, would be less probable because of the tightness of the transition states. In this view C_2H_4 must come from C_2H_5 dissociation, and all of the data at high temperature should be able to be modeled by considering only atomic dissociation.

In this paper we have used the H-atom ARAS technique to observe the methyl reactions after initial formation from the fast dissociation of CH_3I. The experiment is therefore similar to that of Frank and Braun-Unkhoff. [14] It is not however a repeat of their study because the presently used photometer system is substantially more sensitive. Thus, data can be obtained with much less source concentration, at both higher and lower temperatures, thereby diminishing the effects of secondary reactions. Hence, the present results can be viewed as an extension of the Frank and Braun-Unkhoff, [14] Roth and Just, [11] and Roth [12] data.

EXPERIMENTAL

Apparatus: The present experiments were performed with a shock tube operating in the reflected mode. It has been previously described. [20] Between each experiment, the tube was routinely pumped to $<10^{-8}$ Torr by an Edwards Vacuum Products, Model CR100P, packaged pumping system. Eight pressure transducers (PCB Piezotronics, Inc., Model 1132A), placed at fixed intervals towards the end of the tube,

were used to determine the incident shock velocity. Final temperature and density for each experiment were determined from the incident velocity of the shock front and the initial thermodynamic conditions. Corrections for non-idealities due to boundary layer formation were subsequently applied. [20, 21] The photometer system was radially located 6 cm from the endplate and had an optical path length of 9.94 cm. An EMR G14 solar blind photomultiplier tube was used to measured transmittances from the resonance lamp. Transmittances and the differentiated signals from the pressure transducers were recorded with a dual-channel (Nicolet 4094C) digital oscilloscope. Gas mixtures and reactant pressures were measured with an MKS Baratron capacitance manometer.

H-atom Detection: The atomic resonance absorption spectroscopic (ARAS) technique was used to monitor H-atom formation. As in all earlier H-atom work from this laboratory, [22-27] the lamp was operated at 40 watts microwave power and 2 Torr of prepurified He. An atomic filter section was additionally used to establish the fraction of non-$Ly_{\alpha\text{-}H}$ light. Sufficient H-atom residual H_2 and CH_4 are present to give an easily measured signal through an O_2 (1 atm of dry air) gas filter. Under these conditions, the lamp is insignificantly reversed, and a Doppler broadened calculation at an equivalent lamp temperature of 480 K with the known oscillator strength for $Ly_{\alpha\text{-}H}$ will give an exact relationship between absorbance, ABS= -lnT, and [H], [22, 23] and this relationship is nearly linear above ~700K and $T = I/I_0 \geq 0.1$.

Experiments have been performed here to show that this procedure is accurate. Steady-state levels of [H] formed from two reactions have been measured and used for calibration. Herzler and Frank [28] have previously used $C_2H_5 + M \rightarrow C_2H_4 + H + M$ (C_2H_5 formed from the thermal decomposition of C_2H_5I) as a source of H-atoms and have shown, from concurrent I-atom ARAS observations, that the secondary chemistry is relatively unimportant at low initial concentrations. Under their conditions they also indicated that molecular elimination to give HI should be <0.2 of the total decomposition; otherwise the H + HI reaction would affect their measured profiles. The results of our

experiments (1481-2020 K) with C_2H_5I are shown in Fig. 1a. The ordinate values are determined from line absorption calculations at the temperatures of the experiments. With the assumption of one H-atom per dissociation (i. e., elimination to give HI has zero rate), the slope of the line in the figure should be unity whereas the actual value is (0.80 ± 0.03). Hence, our most pessimistic conclusion is that the line absorption calculational method can at most be in error by ~+20%; however, if HI elimination occurs then this error is less. In the other set of calibration experiments we used the $Cl + H_2 \rightarrow H + HCl$ reaction. The Cl-atom source was $COCl_2$. In earlier experiments we established that 1.81 Cl-atoms were formed for every one molecule dissociated (i. e., 9.5 % of the reaction occurs through molecular elimination to give Cl_2). [29] Figure 1b shows the results of ten experiments between 1784-2381 K where the ordinate values are determined from the above mentioned line absorption calculations. The slope of the linear least squares line is (0.99 ± 0.03). These two calibrations show that accurate absolute values of [H] can be determined from line absorption calculations, (probably better than from these two chemical methods) simply because the oscillator strength for $Ly_{\alpha\text{-}H}$ is theoretically better known than for those of any other transition in the entire field of spectroscopy.

Kinetics Experiments: Thirty-four experiments have been performed between 1224-2520 K with CH_3I as the methyl-radical precursor. Figure 2a shows a typical raw data signal from which a plot of $[H]_t$ against time can be constructed by converting (ABS) to [H] through a line absorption calculation at the exact temperature of the experiment. The raw data shown in Fig. 2a gives the H-atom profile in Fig. 2b. It should be noted that use of a near Doppler line source gives substantially more sensitivity for H-atoms than used in earlier ARAS studies on the present system. [11,12,14] Since the method is sensitive, it was necessary to carry out blank experiments with Kr because even research grade Kr contains small amounts of H_2 and CH_4. For $T \leq 2520$ K, the rate of formation of H-atoms from these sources was less than 15% of that due to the added

CH_3I. This observation did however place an upper limit on the temperature range of the present study.

Gases: The high purity He (99.995%), used as the driver gas, was obtained from Air Products and Chemicals, Inc. Scientific grade Kr (99.997%), used as the diluent gas in reactant mixtures, was obtained from MG Industries. Airco Industrial Gases supplied the ultra-high purity grade He (99.999%) used in the resonance lamp and the high purity H_2 (99.995%) used in the atomic filter. Analytical grade CH_3I (99%) and C_2H_5I (99%) were obtained from Aldrich Chemical Co. Inc. Both compounds were purified by bulb-to-bulb distillation, retaining for use only the middle thirds.

RESULTS AND DISCUSSION

The present experiments were carried out with quite low $[CH_3I]_0$ (between 0.74 and 3.69 x 10^{13} molecules cm^{-3}) and low density (1.24 to 3.21 x 10^{18} molecules cm^{-3}) so that the secondary chemistry is not too complicated. In order to fit the measured $[H]_t$ for a given experiment, it was necessary to assess the importance of subsequent reactions. A numerical simulation with the known decomposition rate for CH_3I [30] coupled with the chemical mechanisms used by Roth and Just [11] or Frank and Braun-Unkhoff [14] was carried out for the experiment shown in Fig. 2. The result of this simulation is given in Fig. 3. Under most experimental conditions, the simulations showed (a) that CH_3 was almost instantaneous produced, (b) that [H] was formed almost linearly with time, (c) that CH_3 decreased by only 10-20%, and (d) that almost no C_2H_6 was formed, over the time period of the experiments. Initial rate constant estimates for $2CH_3 \rightarrow C_2H_5 + H$ could then be roughly calculated from measured rates, $\Delta[H]/\Delta t$, as: $k = 0.5\ (\Delta[H]/\Delta t)\ (1/0.9[CH_3I]_0)^2$. In numerical integrations with the mechanism shown above the dashed line in Table 1, k_5 in the table was then parametrically refined by more extensive data fitting. This mechanism uses fewer reactions than the earlier studies [11,12,14] because many of the included processes are unimportant due to the lower $[CH_3I]_0$ used here.

Also, molecular elimination is excluded for reasons given in the introduction. With only the partial mechanism of Table 1, the refined results for k_5 from the thirty-four experiments between 1224-2520 K were determined, and these are plotted in Arrhenius form in Fig. 4. The results of Roth and Just [11] and Frank and Braun-Unkhoff [14] are also shown for comparison, and it is apparent that the present results are nearly exactly the same as those of Roth and Just and are only ~20% lower than those of Frank and Braun-Unkhoff, over the respective temperature ranges. With the partial mechanism, however, the derived rate constant at high temperatures becomes strongly non-Arrhenius. The question then arises as to whether strong curvature for k_5 is reasonable. The answer is clearly no because the back reaction would then have to have a rate constant many times faster than the collision rate for H + C_2H_5. Clearly, other H-atom producing reactions become important above ~2000 K, and Roth et al. [8] and Frank and Braun-Unkhoff [14] have identified the source as being due to CH_3 dissociation.

Recently, experiments have been performed by Dean and Hanson [36] and Markus, Woiki, and Roth [37] in which CH-radical, [36, 37] C-atom, [36] and H-atom [37] concentration profiles have been measured in hydrocarbon pyrolysis experiments. The respective temperature ranges were 2500-3800 K and 2100-3000K. In both studies the profiles could be explained by including the cracking reactions of CH_3, CH_2, and CH, reactions (9), (10), and (12)-(14) of Table 1. In our simulations, rate constants from either of these two studies were acceptable but seemed to underestimate the importance of molecular elimination. Kiefer [18, 38] has questioned the relative branching ratios between atomic and molecular elimination processes in both CH_3 and CH_2 decompositions on thermochemical grounds. Use of the Kiefer and Kumaran [18] rate constants gave predicted H-atom rates were that were high, and we therefore carried out our own theoretical estimates.

It is certainly true that both decompositions, CH_3 and CH_2, will be in the low pressure limit above 2000 K so that it is only necessary to evaluate the limiting low pressure rate constants. Theoretical calculations of k_{sc}^0 with the semi-empirical Troe method [39–41] were made using JANAF thermochemical parameters [42] We can agree with Kiefer and Kumaran's CH_3 cracking rate constants to within <20% if the energy transfer parameter, ΔE_{down} = 625 cm^{-1} (i. e., $-\Delta E_{all} \cong$ 112 cm^{-1}) instead of their value of $-\Delta E_{all}$ = 150 cm^{-1}. Our predicted branching ratio between molecular elimination to atomic dissociation in CH_3, reactions (10) to (9), is 0.886 exp(1718 K/T) for 2000-2500 K and is not much different than Kiefer and Kumaran's estimate, 0.87 exp(1334 K/T), for a somewhat higher temperature range. Our value is likewise similar to that of Wagner [43] who has fitted the lower temperature results for the back reactions, CH_2 + H and CH + H_2, with $-\Delta E_{all}$ = 50 cm^{-1}. [44] This prediction at 2000 and 2500 K gives ratio values of 3.3 and 2.0, respectively, whereas the present inferences are 2.1 and 1.8. None of these theoretical values, which are mostly dependent on the differences in the endothermicities for the two channels, agrees* with the experimentally derived values for the branching ratio; [36, 37] however, Kiefer and Kumaran [18] have used their ratio and absolute rate constants to successfully fit some of the Dean and Hanson [36] profiles. We also carried out theoretical calculations for the CH_2 cracking rate constants, reactions (12) and (13), of Table 1. Our calculations can again agree with Kiefer and Kumaran to within <30%; however, we have to use an energy transfer parameter of ΔE_{down} = 542 cm^{-1} (i. e., $-\Delta E_{all} \cong$ 100 cm^{-1}) in contrast to their reported value of $-\Delta E_{all}$ = 43 cm^{-1}. The predicted branching ratio for molecular elimination to atomic dissociation is 0.413 exp(12489 K/T) showing that molecular elimination is really the only important process at high temperature, and this agrees with the conclusions of Kiefer. [18, 38]

In our final analysis, we again fitted the H-atom profile results for the complete range of conditions using the entire set of rate constants shown in Table 1. Reaction (11)

is an estimate that is based on the isoelectronic process, O + CH_3, and reaction (14) is taken from Kiefer and Kumaran. The CH_2 cracking reactions are taken from our own theoretical estimates and are consistent with Kiefer and Kumaran as noted above. In agreement with Frank and Braun-Unkhoff, [14] we also conclude that atomic production by radical pyrolysis predominates over bimolecular production, reaction (5), above ~2100 K, and therefore, most of the excess H-atom production (see Fig. 4) can be attributed to these pyrolyses. On the other hand, these pyrolyses are of negligible importance below ~1950 K giving <10% of the H-atom yield. We have therefore used only those results between 1224-1938 K to determine the rate behavior for the bimolecular reaction (5). The resulting Arrhenius plot is shown in Fig. 5. The line in the figure is calculated from the linear least squares result,

$$k_5 = (5.25 \pm 1.19) \times 10^{-11} \exp(-7384 \pm 312\ K/T)\ cm^3\ molecule^{-1}\ s^{-1} \qquad (1)$$

This result is in excellent agreement with that of Frank and Braun-Unkhoff [14] who report a value,

$$k_5 = 4.65 \times 10^{-11} \exp(-6840\ K/T)\ cm^3\ molecule^{-1}\ s^{-1} \qquad (2)$$

for the temperature range, 1320-2300 K. Our result is only 15-25% lower than Eqn. (2).

The fitting procedure for CH_3 cracking was then applied to those experiments above 2098 K where the effects of reaction (5) as represented by Eqn. (1) gave <50% of the H-atom yield. We fixed the branching ratio at the theoretical value from our calculations. The derived results for $CH_3 + Kr \rightarrow CH_2 + H + Kr$ are shown in Fig. 6 as an Arrhenius plot along with the experimental results of Dean and Hanson [36] and Markus et al. [37], and the theoretical results from Kiefer and Kumaran [18] and Wagner

[43]. The present experimental results can be represented by the linear least squares equation,

$$k_9 = 4.68 \times 10^{-9} \exp(-42506\ K/T)\ cm^3\ molecule^{-1}\ s^{-1} \quad (3)$$

Eqn. (3) is only valid over the experimental temperature range, 2098-2520 K. The points deviate from the line by ±67% at the one standard deviation level. The values for the molecular elimination path can be calculated from Eqn. (3) by multiplying by 0.886 exp(1718 K/T). If the experimental result, Eqn. (3), is then compared to our theoretical calculation, the collisional deactivation parameter, ΔE_{down}, has to be modified downward. Eqn. (3) can be recovered to within ±14% if $\Delta E_{down} = 437\ cm^{-1}$ (i. e., $-\Delta E_{all} \cong 84\ cm^{-1}$). Extrapolation to the 3000-4000 K range then gives values that are exactly one-half of those of Kiefer and Kumaran. We therefore agree with their point that the apparent activation energy should decrease due to fall-off effects. It is also clear from inspection of Fig. 6 that the present values agree within experimental error to those of both Dean and Hanson [36] and Markus et al., [37] being slightly closer to the latter study. Lastly, the theoretical results of Harding and Wagner [43, 44] are 0.30-0.45 of Eqn. (3). It should be emphasized that the point to this latter theoretical study was to explain the lower temperature data on the back reactions. Using only a single energy transfer parameter, namely $-\Delta E_{all} = 50\ cm^{-1}$, their success was impressive. Hence, with relatively small variations in this energy transfer parameter, their work has demonstrated that all existing data on both forward and back reactions for this system can now be reconciled with theory.

In summary, the present results reinforce the explanation of earlier results on the thermal reactions of CH_3; namely, that the rate constants based on H-atom formation with the ARAS technique contain contributions not only from the C_2H_5 + H reaction but also

from the thermal cracking of CH_3 itself. With the presently used low $[CH_3I]_0$, the reaction can be separated into three relatively well separated regimes. At low temperature and high pressure, recombination to form C_2H_6 is the only important pathway. Because this process involves stabilization with an efficiency factor that decreases with increasing temperature, its importance at pressures of ~1 atm diminishes as temperature increases above ~1250 K. The competitive atomic elimination process then accounts for nearly all of the reactivity up to ~1950 K at which point the pyrolysis of CH_3 then becomes the most important H-atom producing process. The implications of these results on the oxidative modeling of hydrocarbons is unclear because one may have regions, depending on pressure, temperature, and absolute $[CH_3]$, where two or more of these three destruction mechanisms are contributing. Then detailed modeling becomes absolutely essential for explaining the experimental results.

There is an important theoretical implication from Eqn. (1). In an RRK formulation for CH_3 recombination, rate constants based on C_2H_6 formation have the form,

$$k_{recombination} = k_{add} \int_{\varepsilon_o}^{\infty} \frac{\beta\omega\, f(\varepsilon)d\varepsilon}{(kf\varepsilon + kb\varepsilon + \beta\omega)}, \qquad (4)$$

where k_{add}, $k_{f\varepsilon}$, $k_{b\varepsilon}$, β, ω, and $f(\varepsilon)$ refer to the high pressure rate constant for CH_3 self reaction, the specific RRK (or RRKM) rate constant for forward dissociation, the specific RRK (or RRKM) rate constant for backward dissociation at threshold energy, ε_o, the collisional deactivation efficiency, the collision rate constant, and the RRK (or RRKM) normalized distribution function for a given temperature, respectively. This equation shows that the limiting high pressure rate constant should be k_{add}. However, rate constants based on H-atom formation from reaction (5) in Table 1, have the form,

$$k_5 = k_{add} \int_{\varepsilon_o}^{\infty} \frac{k_f\varepsilon f(\varepsilon)d\varepsilon}{(k_f\varepsilon + k_b\varepsilon + \beta\omega)}, \quad (5)$$

implying that at very high temperature and low pressure, the limiting rate constant should again be k_{add}. The A-factor from Eqn. (1) is 5.25 x 10^{-11} cm^3 $molecule^{-1}$ s^{-1} which is near the collision rate constant corrected for the electronic degeneracy ratio. [15] In contrast, recent estimates from Walter et al. [33] suggest decreasing values with increasing temperature. Their extrapolated estimate at 2000 K would be 1.7 x 10^{-11} cm^3 $molecule^{-1}$ s^{-1}. This disagreement requires a continuing theoretical assessment on this important combustion reaction.

Acknowledgment: The authors wish to thank Drs. A. F. Wagner, L. B. Harding, and J. P. Hessler for a thorough reading of the manuscript and helpful suggestions. This work was supported by the U. S. Department of Energy, Office of Basic Energy Sciences, Division of Chemical Sciences, under Contract No. W-31-109-Eng-38.

References

1 Gomer, R, and Kistiakowsky G. B., *J. Chem. Phys.* 19:85–91 (1951).

2 Mallard, W. G., Westley, F., Herron, J. T., Cvetanovic, R. J., and Hampsom, R. J., NIST Chemical Kinetics Database - ver 3.0, NIST Standard Reference Data, Gaithersburg, MD (1991).

3 Tsuboi, T., *Jpn. J. Appl. Phys.* 17:709–xxx (1978).

4 Gardiner, W. C. Jr., Owen, J. H., Clark, T. C., Dove, J. E., Bauer, S. H., Miller, J. A., and McLean, W. J., *Fifteenth Symposium (International) on Combustion*, The Combustion Institute, Pittsburgh, 1975, pp. 857–868.

5 Kern, R. D., Singh, H. J., and Wu, C. H., *Int. J. Chem. Kinet.* 20:731–747 (1988).

6 Hidaka, Y., Nakamura, T., Tanaka, H., Inami, K., and Kawano, H., *Int. J. Chem. Kinet.* 22:701–709 (1990).

7 Chiang, C. C., and Skinner, G. B., *J. Phys. Chem.* 85:3126–3129 (1981).

8 Roth, P., Barner, U., and Loehr, R., *Int. Symp. Shock Tubes Waves Proc.* 12:621–628 (1980).

9 Kiefer, J. H., and Budach, K. A., *Int. J. Chem. Kinet.* 16:679–695 (1984).

10 Roth, P. and Just, Th., *Material Research Symp. Proc.* NBS Spec. Publ. 561, 10:91 (1979).

11 Roth, P. and Just, Th., *Ber. Bunsenges. Phys. Chem.* 83:577–583 (1979).

12 Roth, P., *Forsch. Ingenieurwes.* 46:93–xxx (19xx)

13 Warnatz, J., in *Combustion Chemistry*, W. C. Gardiner, Jr. (Ed.), Springer-Verlag, New York (1984), pp. 197–509.

14 Frank, P, and Braun-Unkhoff, M., *Proceedings of the 16th Symposium on Shock Tubes and Waves,* VCH, Weinheim, 1988, pp. 379–385.

15 Lim, K. P., and Michael, J. V., *J. Chem. Phys.* 98: 3919–3928 (1993).

16 Davidson, D. F., Di Rosa, M. D., Hanson, R. K., and Bowman, C. T., *Int. J. Chem. Kinet.* 25:969–982 (1993).

17 Just, Th., *Proceedings of the 13th International Symposium on Shock Tubes and Waves*, SUNY, Albany, 1982, pp. 54-67.

18 Kiefer, J. H., and Kumaran, S. S., *J. Phys. Chem.* 97:414–420 (1993).

19 Raghavachari, K., Frisch, M. J., Pople, J. A., and Schleyer, P. v. R., *Chem. Phys. Lett.* 85:145–149 (1982).

20 Michael, J. V., *Prog. Energy Combust. Sci.* 18:327–347 (1992), and references cited therein.

21 Michael, J. V., and Sutherland, J. W., *Int. J. Chem. Kinet.* 18:409–436 (1986).

22 Lynch, K. P., Schwab, T. C. and Michael, J. V., *Int. J. Chem. Kinet.* 8:651–671 (1976).

23 Maki, R. G., Michael, J. V., and Sutherland, J. W., *J. Phys. Chem.* 89:4815–4821 (1985).

24 Michael, J. V. and Wagner, A. F., *J. Phys. Chem.* 94:2453–2464 (1990).

25 Michael, J. V., *J. Chem. Phys.* 92:3394–31402 (1990).

26 Shin , K. S. and Michael, J. V., *J. Phys. Chem.* 95:5864–5869 (1991).

27 Shin, K. S. and Michael, J. V., *J. Chem. Phys.* 95:262–73 (1991).

28 Herzler, J. and Frank, P., *Ber. Bunsenges. Phys Chem.* 96:1333-1338.

29 Lim, K. P. and Michael, J. V., *J. Phys. Chem.*, in press.

30 Saito, K., Tahara, H., Kondo, O., Yokubo, T., Higashihara, T., and Murakami, I., *Bull. Chem. Soc. Jpn.* 53:1335–1339 (1980).

31 Equilibrium constant calculated from the molecular parameters given in; Herzberg, G., *Molecular Spectra and Molecular Structure*, Van Nostrand Reinhold, New York, 1966, p. 621.

32 Based on I + CH_4: Golden, D. M., Walsh, R., and Benson, S. W., *J. Am. Chem. Soc.* 87:4053–4057 (1965).

33 Walter, D., Grotheer, H.-H., Davies, J. W., Pilling, M. J., and Wagner, A. F., *Twenty-Third Symposium (International) on Combustion*, The Combustion Institute, Pittsburgh, 1990, pp. 107–114.

34 Hwang, S. M., Rabinowitch, M. J., and Gardiner, W. C., Jr., Chem. Phys. Lett. 205:157–162 (1993).

35 Calculated from forward rates with results by: Böhland, T., Dóbé, S., Temps, F., and Wagner, H. Gg., *Ber. Bunsenges. Phys. Chem.* 89:1110–1116 (1985), and equilibrium constants.

36 Dean, A. J., and Hanson, R. K., *Int. J. Chem. Kinet.* 24:517–532 (1992).

37 Markus, M. W., Woiki, D., and Roth, P., *Twenty-Fourth Symposium (International) on Combustion*, The Combustion Institute, Pittsburgh, 1992, pp. 581–588.

38 Kiefer, J. H., *Twenty-Fourth Symposium (International) on Combustion*, The Combustion Institute, Pittsburgh, 1992, pp. 588.

39 Troe, J., *J. Chem. Phys.* 65:4745–4757 (1977); *ibid.* 4758–4775 (1977).

40 Troe, J., *J. Phys. Chem.* 83:114–126 (1979).

41 Troe, J., *Ber. Bunsenges. Phys. Chem.* 87:161–169 (1983); Gilbert, R. G., Luther, K., and Troe, J., *ibid.* 169–177 (1983)

42 Chase, M. W. Jr., Davies, C. A., Downey, J. R. Jr., Frurip, D. J., McDonald, R. A., and Syverud, A. N., *J. Phys. Chem. Ref. Data* 14:Supplement No. 1 (1985).

43 Wagner, A. F., unpublished results.

44 Wagner, A. F., and Harding, L. B., in *Isotope Effects in Gas-Phase Chemistry* (J. A. Kaye, Ed.), American Chemical Society, Washington, 1992, ACS Symp. Ser. 502, p. 48–63.

Table 1. The Mechanism for the Thermal Reactions of CH_3[a]

1.	$CH_3I \rightarrow CH_3 + I$	$k_1 = \rho \times 4.17 \times 10^{-9} \exp(-21419\ K/T)$[b]
2.	$I + CH_3 \rightarrow CH_3I$	$k_2 = k_1/(2.897 \times 10^{25} \exp(-26203\ K/T))$[c]
3.	$I + CH_3I \rightarrow HI + CH_2I$	$k_3 = 8.32 \times 10^{-10} \exp(-17162\ K/T)$[d]
4.	$CH_3 + CH_3 \rightarrow C_2H_6$	$k_4(T,\rho)$ = from Walter *et al.*,[e] Hwang *et al.*,[f] and Davidson *et al.*[g]
5.	$CH_3 + CH_3 \rightarrow C_2H_5 + H$	k_5 = To be fitted
6.	$CH_3 + CH_3 \rightarrow CH_2 + CH_4$	$k_6 = 1.32 \times 10^{-12} \exp(-7165\ K/T)$[h]
7.	$C_2H_5 \rightarrow C_2H_4 + H$	$k_7 = \infty$
8.	$CH_4 \rightarrow CH_3 + H$	$k_8 = \rho \times 3.16 \times 10^{23}\ T^{-8.11} \exp(-58854\ K/T)$[j]
9.	$CH_3 \rightarrow CH_2 + H$	k_9 = To be fitted
10.	$CH_3 \rightarrow CH + H_2$	$k_{10} = k_9 \times 0.886 \exp(1718\ K/T)$[k]
11.	$CH_2 + CH_3 \rightarrow C_2H_4 + H$	$k_{11} = 1 \times 10^{-10}$[l]
12.	$CH_2 \rightarrow CH + H$	$k_{12} = \rho \times 3.39 \times 10^{-9} \exp(-46100\ K/T)$[k]
13.	$CH_2 \rightarrow C + H_2$	$k_{13} = k_{12} \times 0.413 \exp(12489\ K/T)$[k]
14.	$CH \rightarrow C + H$	$k_{14} = \rho \times 1.66 \times 10^{-10} \exp(-32209\ K/T)$[j]

[a] All rate constants are in molecular units. [b]From ref. 30. ρ is the total density in molecules cm^{-3}. [c]Ref. 31. [d]Ref. 32. [e]Ref. 33. [f]Ref. 34. [g]Ref.16. [h]Ref. 35. [j]Ref. 18. [k]See text. [l]Estimated.

Figures

Fig. 1. The plots are the steady-state yields of [H] as determined from the line absorption calculations versus the initial reactant concentrations in the (a) $C_2H_5 + M \rightarrow C_2H_4 + H + M$ and (b) $Cl + H_2 \rightarrow H + HCl$ studies. See text.

Fig. 2. The top panel displays a typical experimental record showing decreasing ARAS signal as H-atoms are produced from the thermal reactions of CH_3 radicals. The experimental conditions are: T = 1903 K, P = 244 Torr, ρ = 1.240 x 10^{18} cm^{-3}, and X_{CH_3I} = 6.120 x 10^{-6}. The signal is converted to absolute [H] using a specifically calculated curve-of-growth from a line absorption calculation at 1903 K. The H-atom profile is displayed in the bottom panel. The solid line is the [H] yield determined from the full reaction mechanism simulation shown in Table 1.

Fig. 3. A plot of reactant and product profiles from a simulation of the self-reaction of CH_3 radicals based on the mechanism in Table 1. The conditions are the same as in the actual experiment of Fig. 2.

Fig. 4. An Arrhenius plot of the experimentally determined second-order rate constants for the CH_3 self-reaction on the assumption that the [H] yield comes from only reaction (5) of Table 1. Published results from other studies are also plotted for comparison.

Fig. 5 An Arrhenius plot of the rate constants for the CH_3 self-reaction to give H + C_2H_5. The reaction (5) values are determined from fits to the data below 1938 K with the full mechanism of Table 1.

Fig. 6 An Arrhenius plot of the rate constants for the decomposition of CH_3 to give H + CH_2. The reaction (9) values are determined from fits to the data in the temperature range, 2098-2520 K, using the full mechanism of Table 1. Also shown for comparison are earlier experimental [36, 37] and theoretical results. [18, 43].

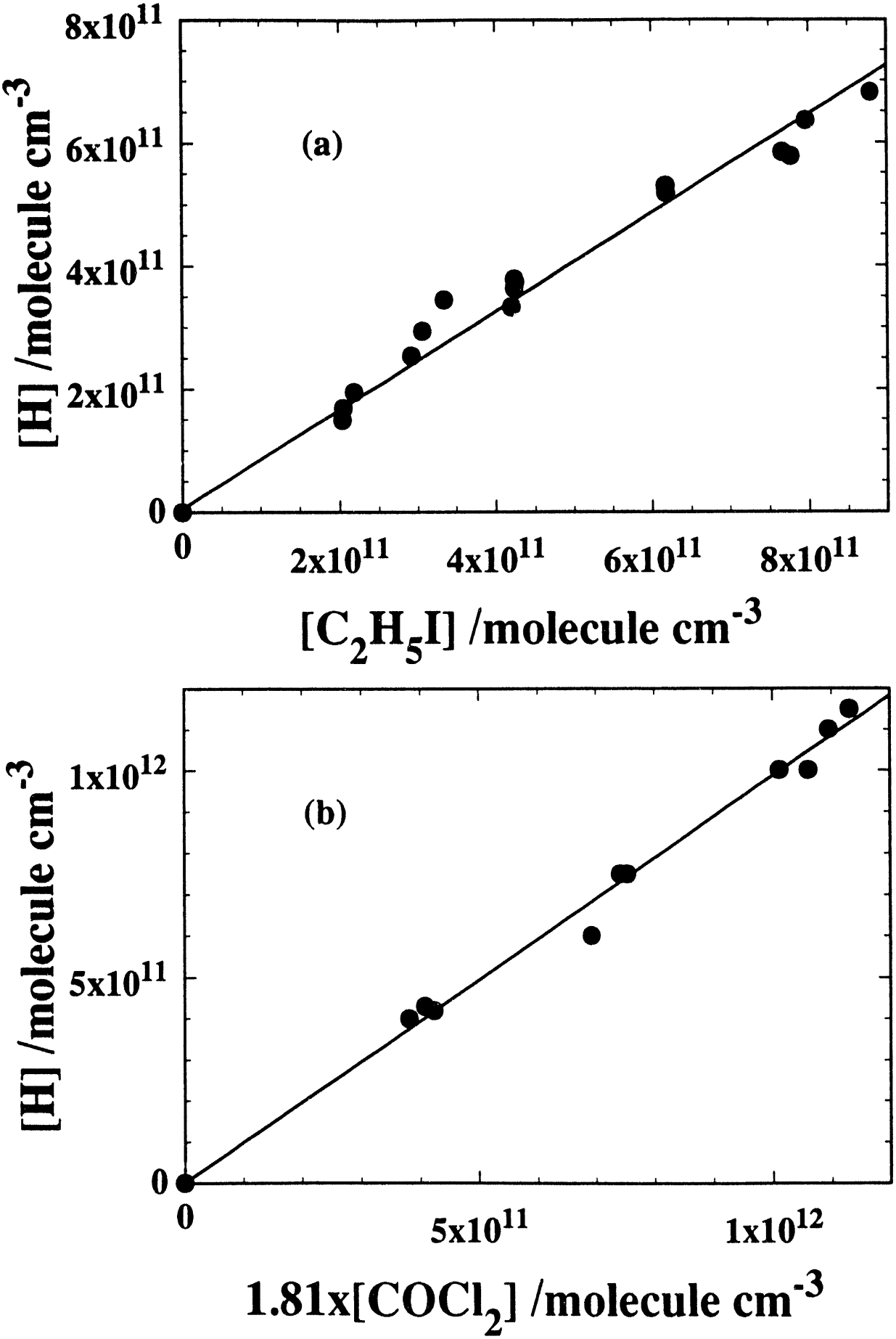
(a)
[H] /molecule cm-3
8x10^11
6x10^11
4x10^11
2x10^11
0
0
2x10^11
4x10^11
6x10^11
8x10^11
[C2H5I] /molecule cm-3
(b)
[H] /molecule cm-3
1x10^12
5x10^11
0
0
5x10^11
1x10^12
1.81x[COCl2] /molecule cm-3

Fig. 1

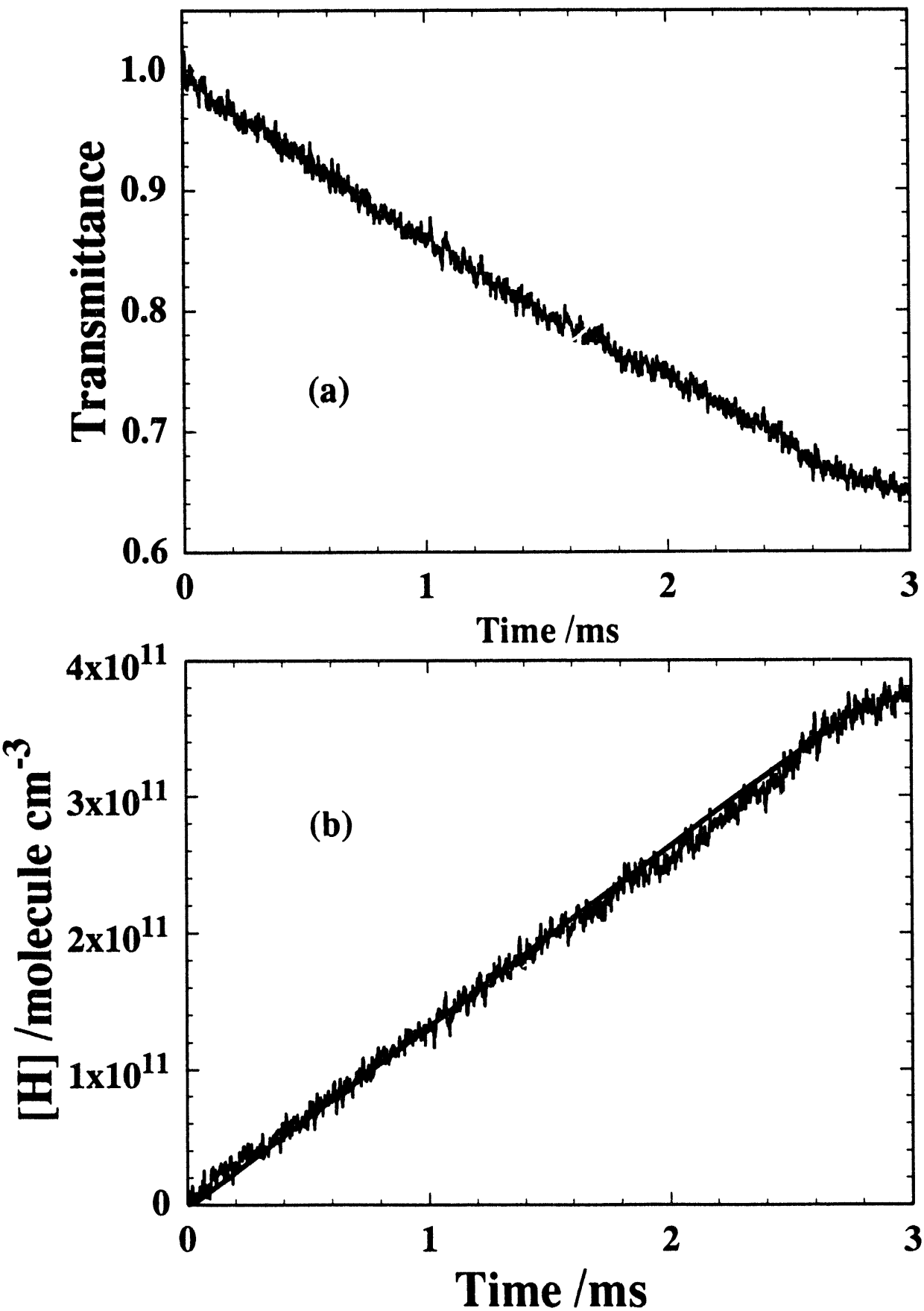
Transmittance
1.0
0.9
0.8
0.7
0.6
(a)
0
1
2
3
Time /ms
[H] /molecule cm-3
4x10^11
3x10^11
2x10^11
1x10^11
0
(b)
0
1
2
3
Time /ms

Fig. 2

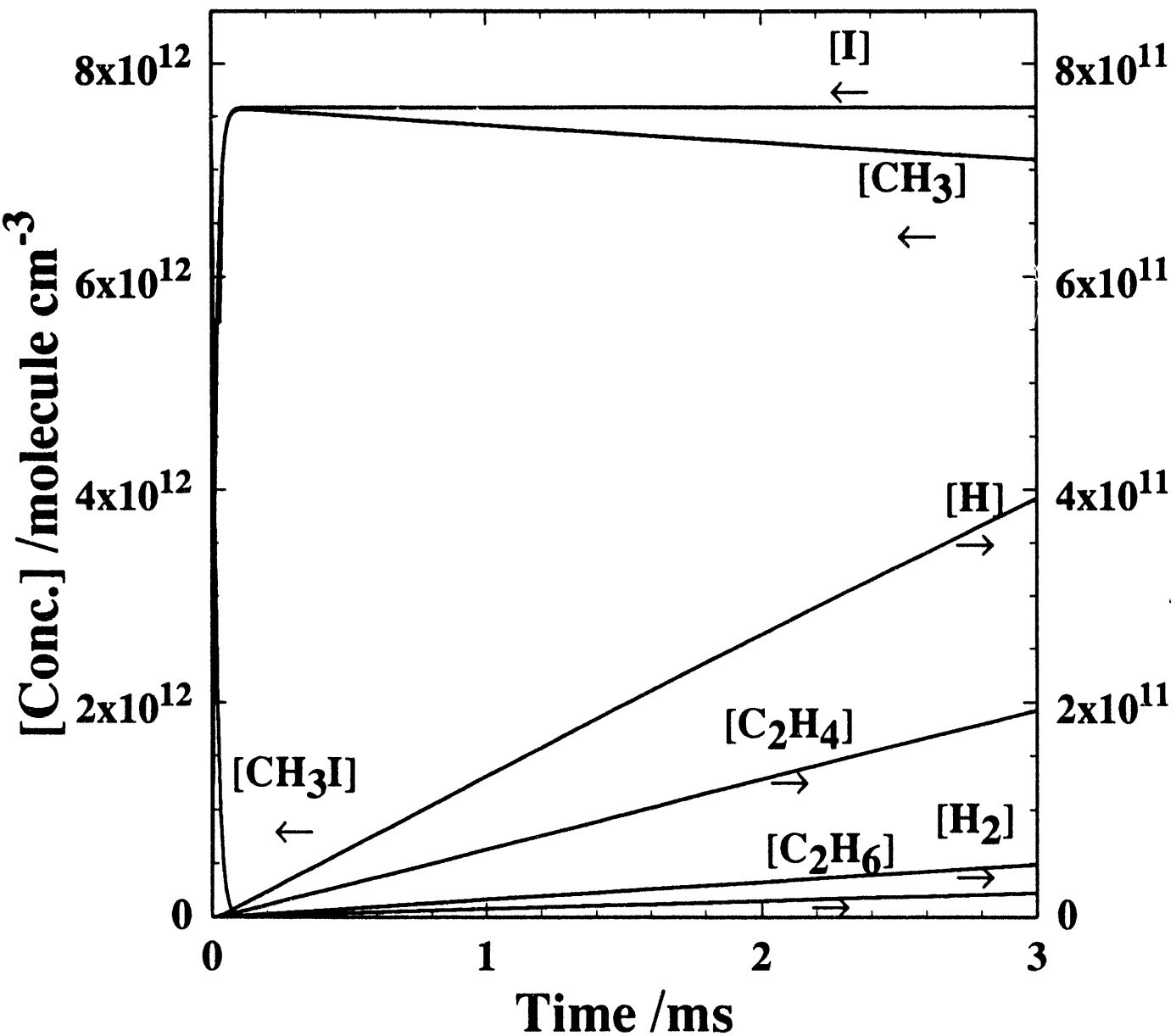
[Conc.] /molecule cm-3
8x10^12
6x10^12
4x10^12
2x10^12
0
8x10^11
6x10^11
4x10^11
2x10^11
0
0
1
2
3
Time /ms
[I]
[CH3]
[H]
[C2H4]
[CH3I]
[H2]
[C2H6]

Fig. 3

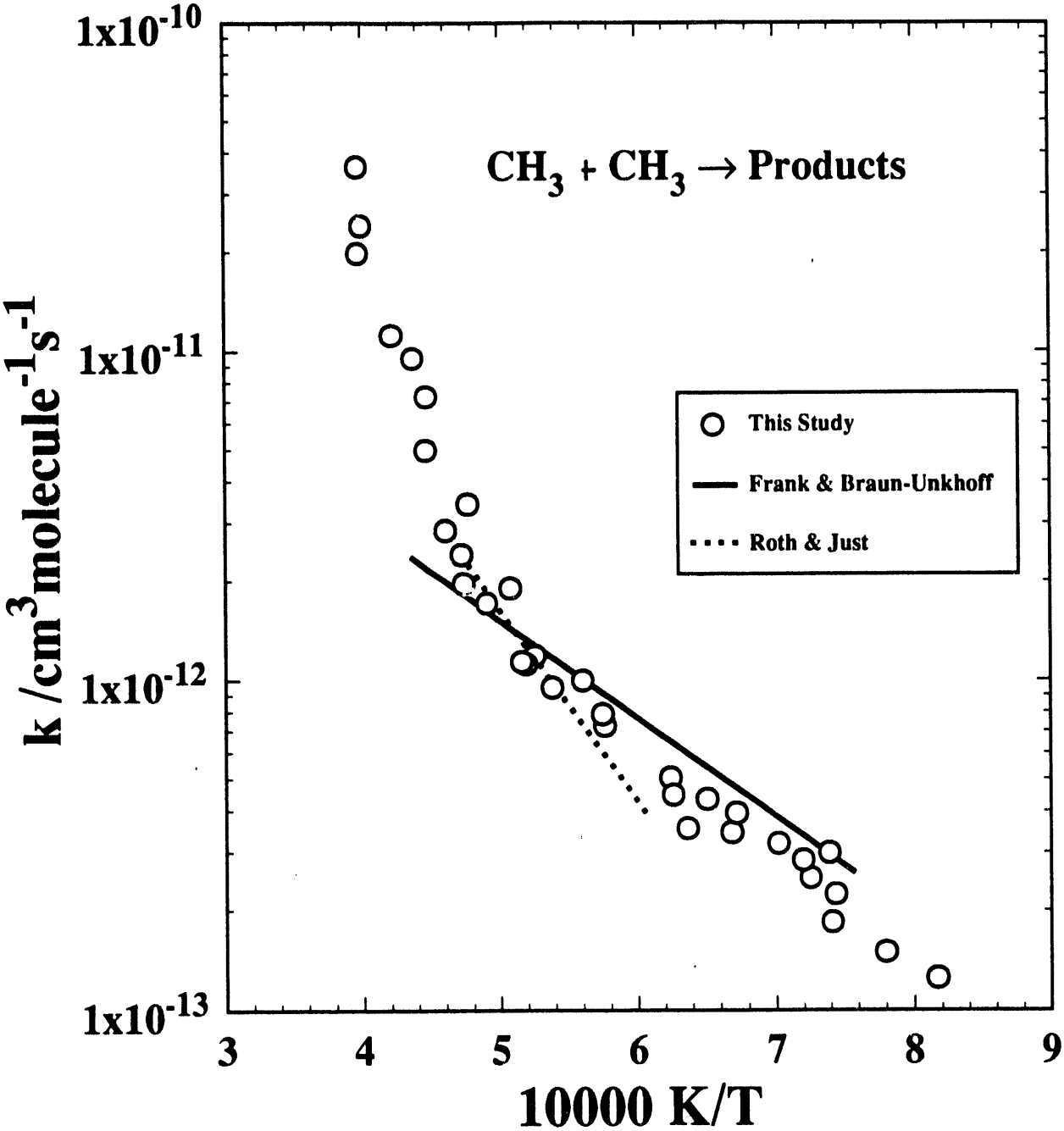
1x10-10
1x10-11
1x10-12
1x10-13
k /cm3molecule-1s-1
CH3 + CH3 → Products
This Study
Frank & Braun-Unkhoff
Roth & Just
3
4
5
6
7
8
9
10000 K/T

Fig. 4

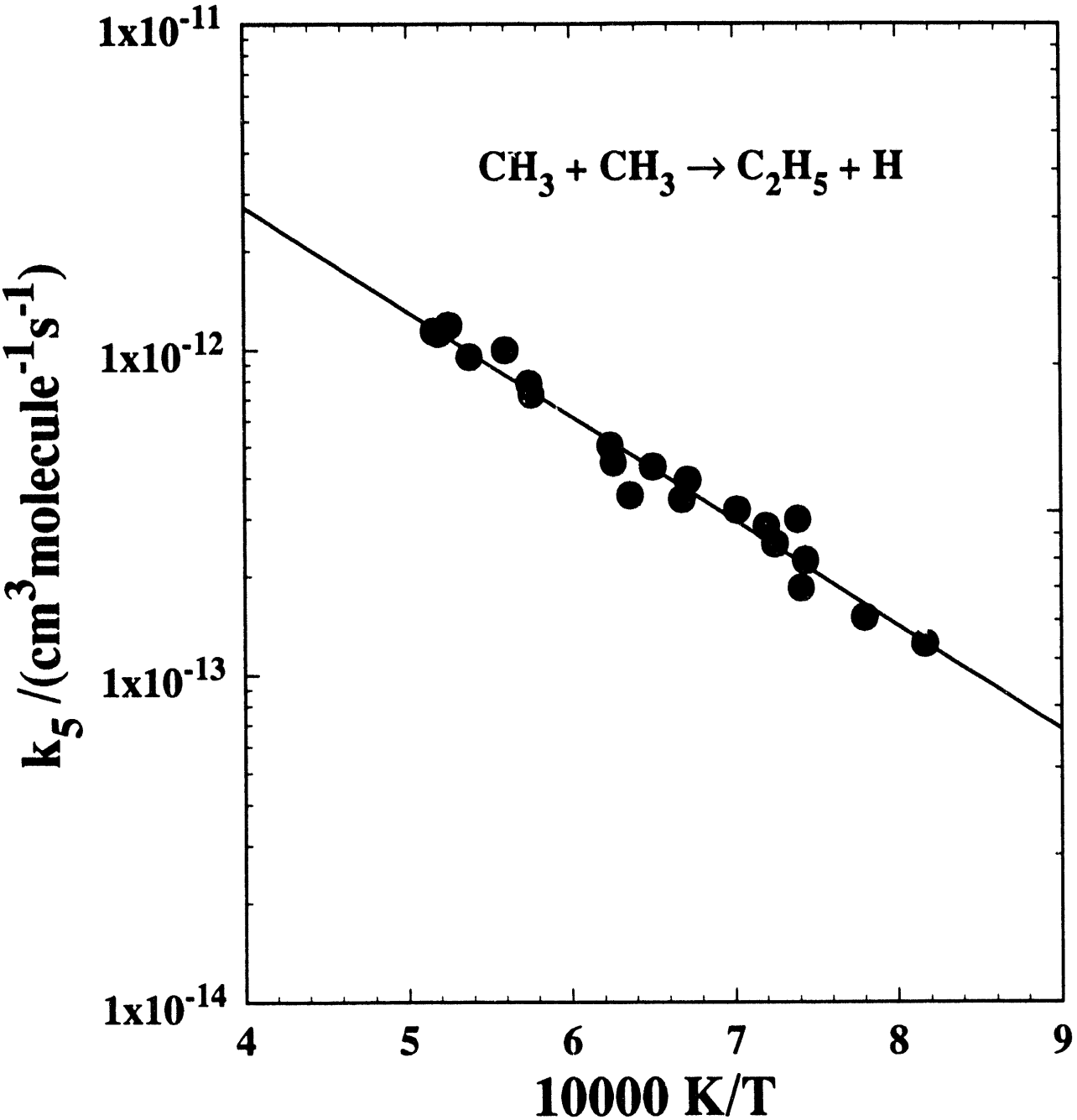
1x10-11
1x10-12
1x10-13
1x10-14
k5 /(cm3molecule-1s-1)
CH3 + CH3 → C2H5 + H
4
5
6
7
8
9
10000 K/T

Fig. 5

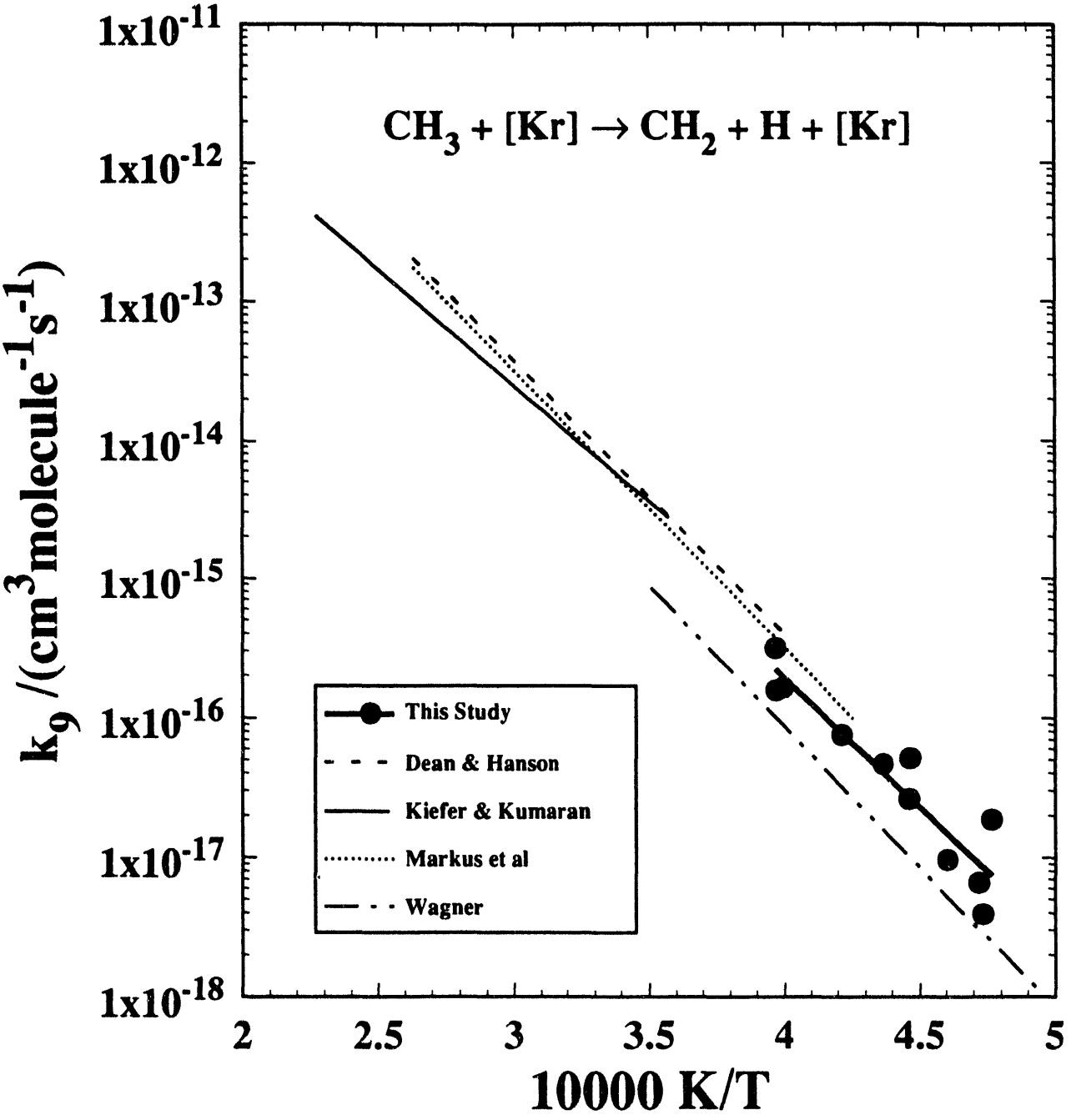
$CH_3 + [Kr] \rightarrow CH_2 + H + [Kr]$
k_9 /($cm^3 molecule^{-1} s^{-1}$)
1x10^{-11}
1x10^{-12}
1x10^{-13}
1x10^{-14}
1x10^{-15}
1x10^{-16}
1x10^{-17}
1x10^{-18}
2
2.5
3
3.5
4
4.5
5
10000 K/T
This Study
Dean & Hanson
Kiefer & Kumaran
Markus et al
Wagner

Fig. 6

DATE

FILMED

7/7/94

END